A Monte Carlo approach to the microdosimetric kinetic model to account for dose rate time structure effects in ion beam therapy with application in treatment planning simulations

(Article begins on next page)

A Monte Carlo approach to the Microdosimetric Kinetic Model to account for dose rate time structure effects in ion beam therapy with application in treatment planning simulations

Lorenzo Manganaro,[*] Roberto Cirio, Federico
Dalmasso, Vincenzo Monaco, and Roberto Sacchi

Physics Department, Università degli studi di Torino, Torino, Italy and

Istituto Nazionale di Fisica Nucleare (INFN), Torino, Italy

Germano Russo,[†] Simona Giordanengo, Anna Vignati, and Andrea Attili

Istituto Nazionale di Fisica Nucleare (INFN), Torino, Italy

Silvia Muraro

Istituto Nazionale di Fisica Nucleare (INFN), Milano, Italy

(Dated: January 23, 2017)

Abstract

Purpose: Advanced ion beam therapeutic techniques, such as hypofractionation, respiratory gating, or laser-based pulsed beams, have dose rate time structures which are substantially different from those found in conventional approaches. The biological impact of the time structure is mediated through the β parameter in the linear quadratic (LQ) model. The aim of this study is to assess the impact of changes in the value of the β parameter on the treatment outcomes, also accounting for non instantaneous intra-fraction dose delivery or fractionation and comparing the effects of using different primary ions.

Methods: An original formulation of the microdosimetric kinetic model (MKM) is used (named MCt-MKM), in which a Monte Carlo (MC) approach was introduced to account for the stochastic spatio-temporal correlations characteristic of the irradiation process and the cellular repair kinetics. A modified version of the kinetic equations, validated on experimental cell survival in-vitro data, was also introduced. The model, trained on the HSG cells, was used to evaluate the relative biological effectiveness (RBE) for treatments with acute and protracted fractions. Exemplary cases of prostate cancer irradiated with different ion beams were evaluated to assess the impact of the temporal effects.

Results: The LQ parameters for a range of cell lines (V79, HSG and T1) and ion species (H, He, C and Ne) were evaluated and compared with the experimental data available in the literature, with good results. Notably, in contrast to the original MKM formulation, the MCt-MKM explicitly predicts an ion and LET dependent β compatible with observations. The data from a split-dose experiment were used to experimentally determine the value of the parameter related to the cellular repair kinetics. Concerning the clinical case considered, an RBE decrease was observed, depending on the dose, ion and LET, exceeding up to 3% of the acute value in the case of a protraction in the delivery of 10 minutes. The intercomparison between different ions shows that the clinical optimality is strongly dependent on a complex interplay between the different physical and biological quantities considered.

Conclusions: The present study provides a framework for exploiting the temporal effects of dose delivery. The results show the possibility of optimizing the treatment outcomes accounting for the correlation between the specific dose rate time structure and the spatial characteristic of the LET distribution, depending on the ion type used.

2

---

* lorenzo.manganaro@unito.it

† Now at EurixGROUP, Via Carcano 26, 10138, Torino, Italy

I. INTRODUCTION

In the last few decades there has been a growing interest toward ion beam therapy due to its attractive features such as a higher conformal dose distribution if compared to photon beams and an increased relative biological effectiveness (RBE) [1, 2]. Nevertheless, the increased RBE of ions also represents a potential disadvantage because of the experimental uncertainty associated with this quantity [3, 4] and the difficulties encountered in modeling it. An incorrect estimation of this parameter could compromise the effectiveness of the whole treatment or even lead to serious side effects. This quantity is closely related to the cellular response and the sensitivity to irradiation, described by the α and β parameters according to the linear quadratic (LQ) model. In this context, a particular importance is assumed by the β parameter, which modulates the biological impact of the dose rate time structure. In fact, according to the LQ formulation, the cell survival can be expressed as:

$$S = \exp(-\alpha\, D - G\, \beta\, D^2) \tag{1}$$

where G represents the generalized Lea-Catcheside factor [5–7] which only depends on the dose rate time structure. Hence, an increase in the cell survival with respect to the acute irradiation is expected when considering protracted or fractionated irradiation, since it gives $G < 1$, and this effect only involves the quadratic term of equation 1 which is modulated by the β parameter.

A dependence of the value of the β parameter on the linear energy transfer (LET) of the radiation and the particle used has been observed by several authors, and a global analysis of all the published *in-vitro* experimental data until 2012 was carried out by Friedrich *et al.* [8] and references therein. This analysis seems to indicate that, irrespective of the cell or ion types, β shows a general decrease with high values of LET. A similar analysis of the the β vs. LET using the same data partitioned in normal and tumor cell was also performed independently by us with similar results and it is reported in the supplementary material (figure S1). On the other hand, several authors report an increasing β with increasing LET [9–12]. However, the behaviour of this parameter as a function of LET is still controversial because of the experimental uncertainty associated with the available data and the difficulties characterizing its measurement. Such an uncertainty is also transferred to the modeling, so that different models predict completely different behaviours of β: exemplary cases are the local effect model (LEM) [13–18], the microdosimetric-kinetic model (MKM) [19–23]

4

and the repair-misrepair fixation (RMF) model [24] which predict a decreasing, a constant
and an increasing β with increasing LET respectively. These models are commonly used in
treatment planning in many facilities all over the world, in particular the LEM has been
used for many years by clinical centers such as GSI, HIT and CNAO [25–28], the MKM
was recently introduced into the clinical practice by the NIRS [29], while the RMF is only
used for research purposes [30]. Moreover, most of the models neglect the β dependence on
the dose rate time structure and consequently they do not take into account the increase in
cell survival observed for dose protraction or fractionation. Therefore, nowadays treatment
plans are made on the assumption that the beams are delivered instantaneously regardless
of the real intra-fraction time structure. Nonetheless, the most advanced ion beam thera-
peutic techniques, such as hypofractionation, respiratory gating, repainting or, looking at
the future, laser-based pulsed beams, have dose rate time structures which are substantially
different from those found in conventional approaches and whose biological impact needs to
be investigated. In this regard, some precursory study have been carried out by Inaniwa *et
al.* [31, 32], who tried to quantify the dose-delivery protraction effect of the irradiation using
the MKM but neglecting the β dependence on LET and limiting the analysis to carbon
ion beams, and by Carabe-Fernandez *et al.* [33] who studied the clinical implications of a
variable β on fractionation and the related variability of the RBE.

The aim of this study is to assess the impact of changes in the value of the β parameter
on the treatment outcomes, also accounting for an arbitrary dose rate time structure and
comparing the effect of using different primary ions. An original formulation of the MKM
(named MCt-MKM) was conceived and implemented to address this issue; in particular, it
was included in a treatment planning system (TPS) and used to evaluate the effect of non
instantaneous intra-fraction dose-delivery in a clinical case of prostate cancer. We remark
that in this clinical study, the only time-dependent radiobiological mechanisms explicitly
modelled are those associated to the repair kinetics of the cell, while other mechanism such
as oxygen effect, tumoral cell repopulation and cell cycle are not accounted for.

II.   MATERIALS AND METHODS

A.   The Monte Carlo temporal-Microsimetric Kinetic Model

At present, one of the most acknowledged radiobiological models is the microdosimetric-kinetic model (MKM), formulated by Hawkins in 1994 [19] as an elaboration of the theory of dual radiation action (TDRA) [34, 35], the repair-misrepair [36] and the lethal-potentially lethal models [37] and then modified over subsequent years [20–23]. Here, an original reformulation of this model is presented, based on a Monte Carlo approach and named Monte Carlo temporal-Microsimetric Kinetic Model (MCt-MKM), that also includes the analytic solution of the kinetic equations formulated by Hawkins and allows to evaluate the temporal effects of the irradiation. The aim of the model is to predict the surviving fraction of cells exposed to ionizing radiation with a completely arbitrary dose rate time structure, where the term "dose rate time structure", is used to indicate the temporal pattern of the dose rate, the latter intended as a function of time in the most general sense; within this definition we consider both the modulations of the dose rate as a function of time due to the fractionation (inter-fraction time), and due to the specific intra-fraction dose delivery, such as single fraction protraction. According to the model hypothesis, the cell survival probability corresponds to the probability that the number of lethal lesions in the cellular nucleus results equal to zero after a large period of time after the irradiation, that is in the limit of the time that increases to infinite. The nucleus is divided into subcellular structures, named *domains*, similar to the *sites* defined in the TDRA and the model is based on the hypothesis that ionizing radiation can cause two kinds of primary lesions in the domain, referred to as type I ($x_I^{(cd)}$) and II ($x_{II}^{(cd)}$) lesions. The rate of production of type I ($\dot{x}_I^{(cd)}$) and II ($\dot{x}_{II}^{(cd)}$) lesions is proportional to the dose rate ($\dot{z}^{(cd)}$), with proportionality constant λ and k respectively; the superscript c and d refer to the specific cell and domain considered. Type I lesions are associated with clustered DNA damages which are directly lethal for the cell, while type II lesions identify non-directly lethal damages that may be repaired with constant rate r, spontaneously converted to irreparable damages with a first-order constant rate a or undergo pairwise combination with other type II lesions in a second-order process with constant rate b. These assumptions led to the formulation of the following kinetic equations

6

that describe the evolution of the number of type I and II lesions inside each domain:

$$\begin{cases} \dot{x}_I^{(cd)} = \lambda\, \dot{z}^{(cd)} + a x_{II}^{(cd)} + b \left(x_{II}^{(cd)}\right)^2 \\ \dot{x}_{II}^{(cd)} = k\, \dot{z}^{(cd)} - (a+r)\, x_{II}^{(cd)} - 2b \left(x_{II}^{(cd)}\right)^2 \end{cases} \tag{2}$$

where $\dot{z}^{(cd)}$ indicates the microscopical dose absorbed by the d-th domain of the c-th cell per unit of time. However, in the case of ion irradiation, the rate of pairwise combination between type II lesions is considered negligible in the evaluation of $\dot{x}_{II}^{(cd)}$ [20, 31, 32] if compared to the first order process (i.e. $2b\left(x_{II}^{cd}\right)^2 << (a+r)x_{II}^{(cd)}$), hence the quadratic term will be neglected in the calculations. As a consequence, equation 2 becomes:

$$\begin{cases} \dot{x}_I^{(cd)} = \lambda\, \dot{z}^{(cd)} + a x_{II}^{(cd)} + b \left(x_{II}^{(cd)}\right)^2 \\ \dot{x}_{II}^{(cd)} \simeq k\, \dot{z}^{(cd)} - (a+r)\, x_{II}^{(cd)} \end{cases} \tag{3}$$

Since the distribution of type I lesions in the nucleus is assumed to be Poissonian, the surviving probability for the c-th cell in the irradiated population can be calculated as

$$S_c = \exp\left(-\sum_{d=1}^{N_D} \lim_{t\to+\infty} x_I^{(cd)}(t)\right) = \exp\left(-\sum_{d=1}^{N_D} \tilde{x}_I^{(cd)}\right) \tag{4}$$

where N_D indicates the total number of domains constituting the cell nucleus. Once defined the dose rate time structure, the quantity $\tilde{x}_I^{(cd)}$ is evaluated by solving the kinetic equations (3).

In the MC computational procedure the choice of cell nucleus and domain geometries are those used by Kase *et al.* [23]. The sensitive volumes of domain and nucleus is cylindrical, the paths of incident ions are parallel to the cylindrical axis and a track segment condition is assumed for the sake of simplifying the calculations. The domains were arranged according to a close packing hexagonal structure inside the nucleus (figure S4, supplementary materials) that is assumed to be water equivalent. The number of domains follows simply from the ratio between the nucleus and domain areas. The sizes of the nucleus and of the domains, reported in table I, have been derived by fitting the experimental data. They are compatible with the ones used in other studies (such as [23]). The corresponding number of domains per nucleus used in the simulations is in the range 106–166 depending on the cell type.

From the point of view of the single domain, the macroscopic irradiation process could be seen as an ordered sequence of interactions between the ions composing the beam and domain itself, where the number of ions, the time of each interaction and the impact parameter of

7

each ion can be sampled from specific probability distributions depending on the dose rate time structure and the kind of irradiation considered. In the most general case of mixed field irradiation, the interacting beam is made of primary ions and fragments with a spectrum of energies. This spectrum is an input for the model and could be evaluated by means of other simulation codes. In particular, we used a monoenergetic spectrum in the comparison with the in-vitro data (see section III A), while, in the case of the treatment plan, we used a complex spectrum (including fragments) derived from the TPS calculations, which in turn is based on FLUKA calculations (see section II B and III C) For each energy and particle type, once defined the imposed macroscopic dose D, the mean number of ions interacting with the nucleus is obtained as:

$$\bar{N}_e = \frac{\rho\,\sigma\,D\,w_e}{\langle \mathrm{LET} \rangle} \tag{5}$$

where σ indicates the cross section, ρ the density of the tissue, the index e refers to the histogram bin of the energy spectrum for each particle type, w_e is the normalized weight of the e-th energy and particle type component of the spectrum, and $\langle \mathrm{LET} \rangle$ the mean LET of the radiation. Hence, the actual number of interacting ions is sampled from a Poissonian probability density function (PDF) with mean value $\bar{N}_e$.

For the evaluation of the single i-th particle contribution to the specific energy per cell and domain, $z_i^{(cd)}$, the MCt-MKM integrates in the domain region the analytical formula for the amorphous track model obtained by a combination of the Kiefer model for the penumbra region [38] and the Chatterjee model for the core radius [39], following the approach of Kase et al. [23]. The spatial coordinates of each particle with respect to the center of the cell are sampled from a uniform PDF.

In the MC simulation the time is implemented by defining, during the initialization phase, a macroscopic time structure for the dose rate to be delivered. At the beginning of the simulation of each cell c, a number of particles is extracted (see equation 5) and, together with the spatial coordinate, a randomly generated temporal coordinate, $t_i^{(c)}$, is also assigned to each one of them. The temporal coordinate is sampled from a temporal PDF that is proportional to the macroscopic dose rate time-function and it is used as an input of the model. The particles are then time-ordered to define a temporal sequence with ordered time indices, so that if $i > j$ then $t_i^{(c)} \geq t_j^{(c)}$. The interaction between the i-th particle and the cell c happens at time $t_i^{(c)}$ and it is assumed to be instantaneous, since its duration is negligible with respect the macroscopic dose rate changes during the irradiation time. The

8

latter assumption allows us to use the α_0 and β_0 parameters that describe the acute local effect (see equation 6) due to the energy deposited by each particle track crossing the cell. Note that, along the irradiation process, each domain is characterized by its own specific random sequence of interactions, in terms of specific energies and time coordinates, which are different from any other domain. One of the benefits of performing a Monte Carlo simulation is that it is possible to evaluate the effect of the irradiation for each domain by considering each specific history, without evaluating averaged quantities in the computation of the effect on the single cell and therefore without the need to introduce correction factors, contrarily to the original MKM formulation. Once the sequences of doses and times for each domain of each cell have been identified via the Monte Carlo, the solution of the kinetic equations (3) (see appendix A) allows us to evaluate the final amount of type I lethal lesions as:

$$\tilde{x}_I^{(cd)} = \frac{\alpha_0}{N_D} \sum_{i=0}^{n_c-1} z_i^{(cd)} + \frac{\beta_0}{N_D} \left(\sum_{i=0}^{n_c-1} z_i^{(cd)} \right)^2 - 2\frac{\beta_0}{N_D} \sum_{i=0}^{n_c-2} \sum_{j=i+1}^{n_c-1} \left(1 - e^{-\frac{1}{\tau}(t_j^{(c)} - t_i^{(c)})} \right) z_i^{(cd)} z_j^{(cd)} \quad (6)$$

where n_c is a Poissonian random variable that indicates the number of particles that interact with the cell c, with an expectation value expressed by equation 5, $\frac{1}{\tau} = (a + r)$ is the time constant that defines the repair kinetics, α_0 and β_0 are the parameters of the model that represent the acute local effect and the indexes i and j refer to the interaction of i-th and j-th particle respectively. Equation (6) could be recast by defining a microscopic local Lea-Catcheside G factor [5, 7] for each cell c and domain d

$$G_{cd} = 1 - \frac{2}{\left(\sum_{i=0}^{n_c-1} z_i^{(cd)} \right)^2} \sum_{i=0}^{n_c-2} \sum_{j=i+1}^{n_c-1} \left(1 - e^{-\frac{1}{\tau}(t_j^{(c)} - t_i^{(c)})} \right) z_i^{(cd)} z_j^{(cd)} \quad (7)$$

that allows us to write:

$$\tilde{x}_I^{(cd)} = \frac{\alpha_0}{N_D} \sum_{i=0}^{n_c-1} z_i^{(cd)} + G_{cd} \frac{\beta_0}{N_D} \left(\sum_{i=0}^{n_c-1} z_i^{(cd)} \right)^2 \quad (8)$$

reproducing the LQ correlation between the total absorbed dose and the number of lethal events. The survival probability for the single cell is evaluated by substituting the (8) in the (4) and the computation of the final surviving fraction is made by averaging S_c over the entire cell population:

$$S = \langle S_c \rangle_c = \left\langle \exp \left(-\sum_{d=1}^{N_D} \tilde{x}_I^{(cd)} \right) \right\rangle_c . \quad (9)$$

9

This allows us to reproduce via the Monte Carlo a complete survival curve by varying the imposed dose. In our simulations, values of imposed dose ranging from 1 to 6 Gy were used. The dose absorbed by each cell fluctuates around the imposed dose due to the MC approach, while the average dose over the cell population converges to the imposed dose. This fluctuation is wider for higher doses due to the Poissonian statistics (equation 5). The corresponding LQ parameters can be obtained by fitting the simulated survival curves, as shown in figure 1.
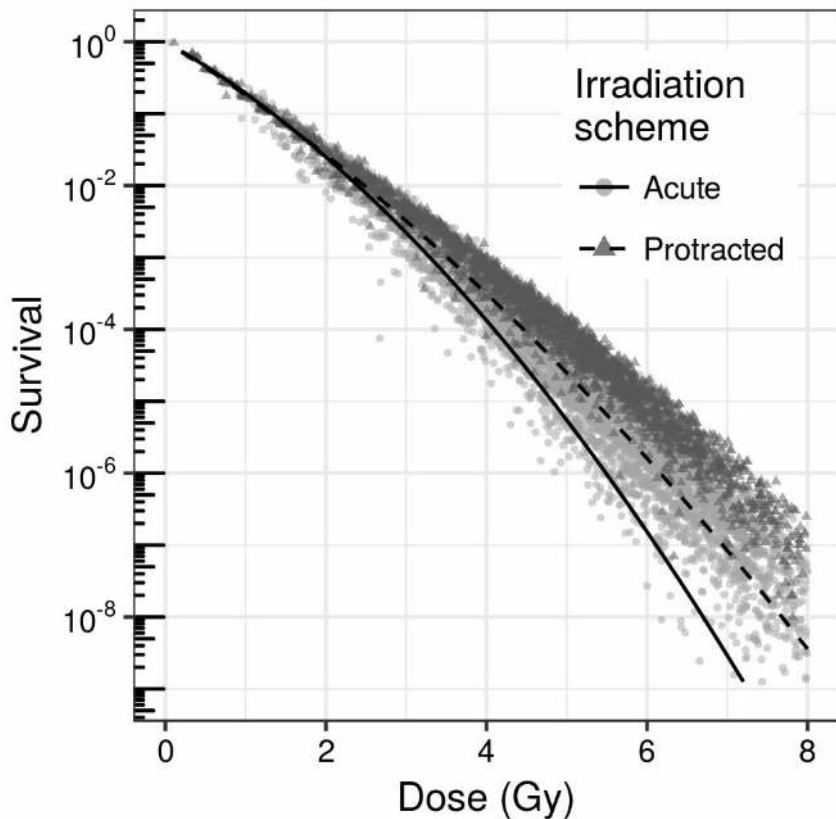

Figure 1. Simulated survival curves obtained for acute (light gray circles) and 30 min protracted (dark gray triangles) monoenergetic (23.8 MeV/u) carbon ion irradiation with imposed doses ranging from 1 to 6 Gy (step: 1 Gy). The dots represent the values of cell survival (a dot for each simulated cell); the variability of the delivered dose with respect to the imposed dose derives by the MC simulation. The two curves were fitted using the LQ model (solid and dashed lines respectively) in order to get the LQ parameters.

An implementation of the MCt-MKM was included in a software developed by the INFN (Istituto Nazionale di Fisica Nucleare), which also provides the implementation of a number

of radiobiological models and offers a useful simulation tool. The software is open source and available on the web (https://github.com/batuff/Survival). Here, the reader interested can find the full code used to produce the presented results.

B. Treatment planning

The MCt-MKM was included in the treatment planning system (TPS) Rplanit (https://github.com/planit-group/Rplanit), an extension of the original TPS PlanKIT [40] developed by the INFN in collaboration with the IBA (Ion Beam Applications S.A.). This TPS incorporates a modeling approach, the beamlets superposition (BS) model, specifically conceived to allow the simulation of beams of different ion types and complex energy spectra, including the nuclear fragmentation that produces a progressive build-up of secondary ions along the penetration depth in the tissue. Track distributions have been generated using Monte Carlo (FLUKA [41]) simulations in a water phantom irradiated with monoenergetic beams. These distributions, collected in look-up tables, are then recombined in the patient geometry using the BS approach and a water equivalent path length approximation. This allowed us to evaluate the biological effect accounting for the complete particle spectrum. We made different treatment plans for a patient with prostate cancer applying the MCt-MKM with the HSG parametrization (table I) and comparing the outcomes in using different primary ions, namely H, He, Li and C. All plans are made using two lateral opposing fields, with a total prescribed RBE weighted dose of 3 Gy(RBE) uniform in the whole planning target volume (PTV). To show the effect of the dose rate time structure, the plans were re-evaluated considering a protraction in the delivery of 10 minutes.

III. RESULTS

A. Acute irradiation

We validated the model through the comparison with the *in vitro* survival experimental data collected in the Particle Irradiation Data Ensamble (PIDE) by Friedrich *et al.* [8]. We used the data of *in vitro* HSG (Human Salivary Gland), V79 (Chinese hamster lung cells) and T1 (Human lymphoblast cells) neoplastic cells exposed to acute irradiation under aerobic conditions of H, He, C and Ne ion beams to examine the MCt-MKM calculation in

11

comparison with the original MKM prediction. Figures 2, 3 and 4 show the LQ parameters α and β dependence on LET for the HSG, V79 and T1 cellular lines respectively comparing experimental and simulated data.
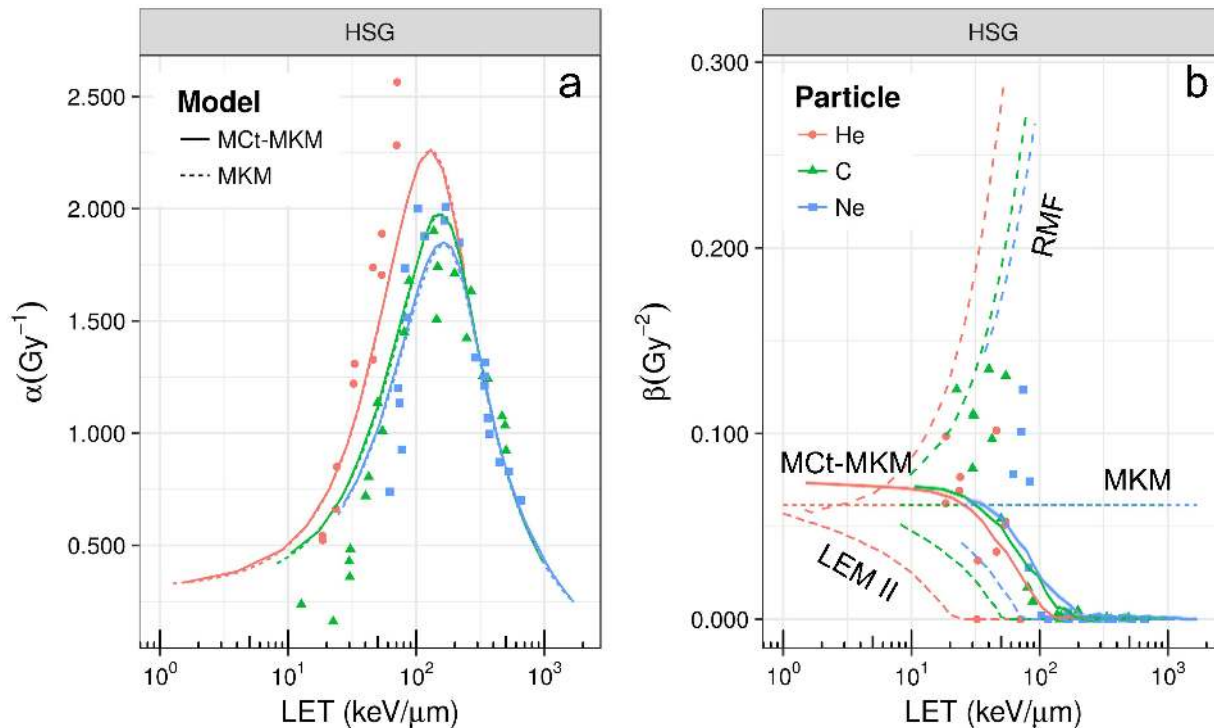

Figure 2.   Linear quadratic α (panel a) and β (panel b) parameters as a function of LET for the irradiation of HSG cells with different ions. Points represent experimental data taken from PIDE [8], different colors/gray levels and shapes refer to He, C and Ne ions respectively (the colour/gray level and shape legend refers both to panel a and b). In panel a, solid and dashed lines represent respectively the extrapolation with the MCt-MKM and the original MKM models, while in panel b a comparison between different model is reported (namely MKM, MCt-MKM, LEM-II and RMF). In the case of the MCt-MKM, overlapped to the α and β curves the MC statistical confidence bands (68%) are reported. These bands are small due to the high statistics and they blends with the curves thickness.

260

The model parameters used in the MCt-MKM calculation are summarized in table I. These were optimized on the experimental data collected in the PIDE considering at the same time all the ions available for the same cell line. In particular the HSG cells, used in the treatment planning, were optimized considering simultaneously α, β, RBE and RBE_{10}, while
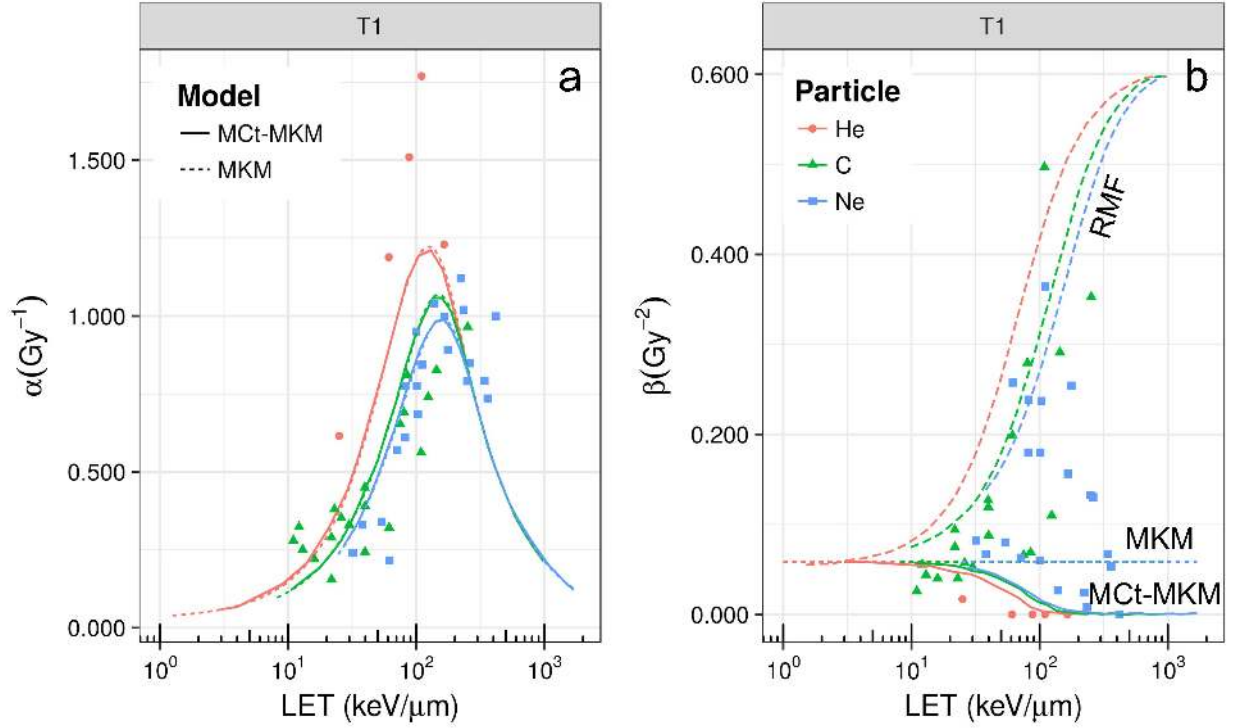
Figure 3. Linear quadratic α (panel a) and β (panel b) parameters as a function of LET for the irradiation of T1 cells with different ions. Points represent experimental data taken from PIDE [8], different colors/gray levels and shapes refer to He, C and Ne ions respectively (the colour/gray level and shape legend refers both to panel a and b). In panel a, solid and dashed lines represent respectively the extrapolation with the MCt-MKM and the original MKM models, while in panel b a comparison between different model is reported (namely MKM, MCt-MKM, LEM-II and RMF). In the case of the MCt-MKM, overlapped to the α and β curves the MC statistical confidence bands (68%) are reported. These bands are small due to the high statistics and they blends with the curves thickness.

in the case of V79 and T1 cells we considered only the LQ parameters. Figures 2, 4 and 3 also report a comparison between different models. In particular panel a shows the comparison between the MKM and the MCt-MKM, evaluated with the same parameter (table I), which predict the same behaviour for α. Panel b shows the comparison between the MKM [23], MCt-MKM (table I), LEM-II ([16]) and RMF [24] models, evaluated with the parameters found in their reference paper respectively. A summary of the χ^2 values obtained for each model can be found in the supplementary materials (table S I). Such an analysis seems to
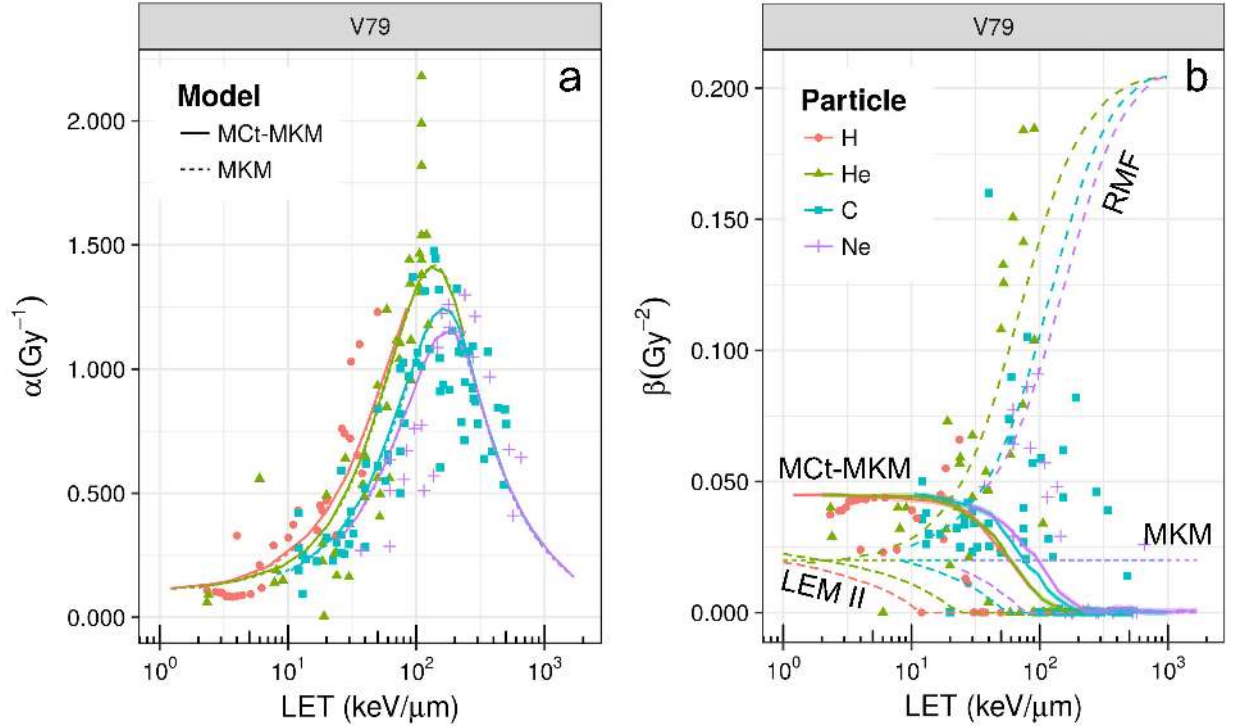
Figure 4. Linear quadratic α (panel a) and β (panel b) parameters as a function of LET for the irradiation of V79 cells with different ions. Points represent experimental data taken from PIDE [8], different colors/gray levels and shapes refer to H, He, C and Ne ions respectively (the colour/gray level and shape legend refers both to panel a and b). In panel a, solid and dashed lines represent respectively the extrapolation with the MCt-MKM and the original MKM models, while in panel b a comparison between different model is reported (namely MKM, MCt-MKM, LEM-II and RMF). In the case of the MCt-MKM, overlapped to the α and β curves the MC statistical confidence bands (68%) are reported. These bands are small due to the high statistics and they blends with the curves thickness.

indicate a better capability of the MCt-MKM to reproduce the experimental behaviour with respect to the other models considered.

B.   Non-acute irradiation: The G factor

We used the data of a *split-dose* experiment carried out by Inaniwa *et al.* [31] to experimentally define the value of the temporal constant τ (equation 7) characteristics of the cell repair kinetics. The experiment consists of the evaluation of the surviving fraction of HSG

14

Table I. MCt-MKM parameters optimized on the experimental data from the PIDE (Particle Irradiation Data Ensamble). For each cell line considered α_0, β_0, the nucleus radius R_n and the domain radius R_d are reported.

Cell Line	α_0 (Gy^{-1})	β_0 (Gy^{-2})	R_n (μm)	R_d (μm)
HSG	0.312	0.073	4.611	0.365
V79	0.104	0.045	3.748	0.364
T1	0.137	0.019	3.694	0.288

cells exposed to carbon ion irradiation (290 MeV/u) with two identical fractions of 2.5 Gy separated by a time interval varying from 0 to 9 hours. The experimental curve (figure 5) was interpolated using equation 7, obtaining:

$$\tau = (23 \pm 3) \; min$$

The band around the fitted curve in figure 5 indicates the sensibility of the survival correspondent to a fluctuation of $\frac{1}{\tau}$ between $\pm 20\%$.

The MCt-MKM was used to investigate the effect of the dose rate time structure in terms of cell survival and its effect on the radiobiological α and β parameters. Some simulations were performed considering different ions (H, He and C) irradiating different cell populations (HSG, T1 and V79) both in acute and non-acute conditions. For each simulation, the difference between the radiobiological parameters identified in acute and non-acute condition was evaluated by means of the standard normal Z-score:

$$Z_x = \frac{|x_{Acute} - x_{Non-Acute}|}{\sqrt{\sigma^2_{x_{Acute}} + \sigma^2_{x_{Non-Acute}}}} \tag{10}$$

where x represents the parameter considered (α or β). Figure 6 shows that the dose rate time structure modulates only the quadratic β parameter keeping unchanged the linear one, but that the modulation decreases with increasing LET. Hence, depending on the ion and cell type, it could be expected that the temporal effect becomes negligible for sufficiently high LET. This allows us to evaluate a macroscopic Lea-Catcheside G factor as:

$$G = \frac{-\ln \langle S_c \rangle_c - \alpha D}{\beta D^2} \tag{11}$$

where $\langle S_c \rangle_c$ represents the average cell survival over the entire cell population, D the total dose delivered while α and β represent the LQ parameters obtained in acute conditions.
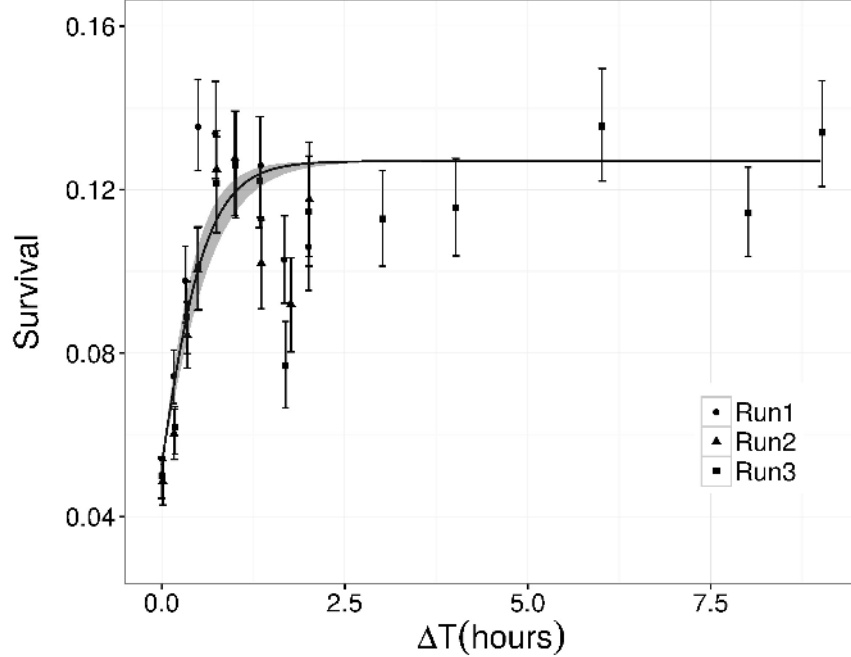
15

Figure 5. Surviving fraction as a function of time between fractions in a split dose experiment. Points represent experimental data taken from Inaniwa *et al.* [31], different shapes indicate different data acquisitions. The band around the solid line corresponds to the fluctuation of $\frac{1}{\tau}$ between $\pm 20\%$.

We found that G does not depend on LET or ion type but it is completely defined by the dose rate time structure. Such a G factor is compatible and analytically definable as a first order repair kinetics with the same time constant defined at the microscopic domain level (equations 3 and 7). This is shown in figure 7 where a comparison between the simulated G factor and its macroscopic analytical definition as a function of the fraction delivery time is reported in the case of protracted and fractionated irradiation respectively. In particular, the analytical expressions used were:

$$G = \frac{2}{(\frac{1}{\tau}T)^2}(e^{-\frac{1}{\tau}T} - 1 + \frac{1}{\tau}T) \tag{12}$$

in the case of protracted irradiation, where T indicates the delivery time, and

$$G = 1 - \frac{2}{N^2}\sum_{i=1}^{N-1}\sum_{j=i+1}^{N}(1 - e^{-\frac{1}{\tau}\Delta t_{ij}}) \tag{13}$$

in the case of fractionation, where N indicates the total number of fractions and Δt_{ij} the distance between the i-th and the j-th fractions.
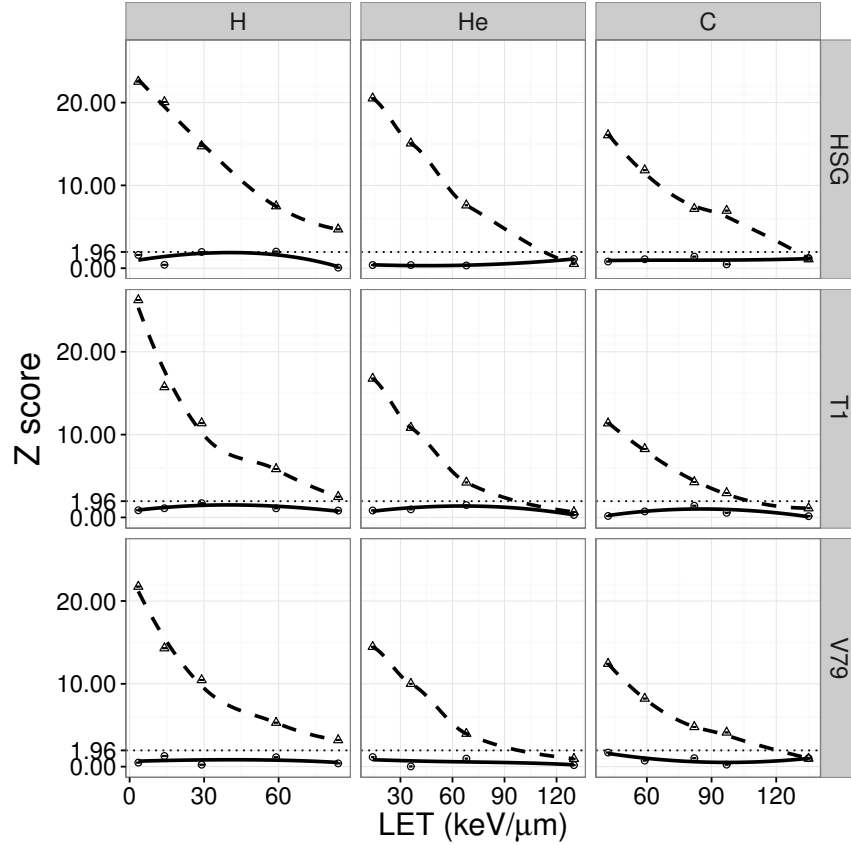
16

Figure 6.   Z-score for the α and β parameters, comparing acute and non-acute irradiations for different cell lines (HSG, T1 and V79) and different ion types (H, He and C). Points represent the values obtained via the Monte Carlo (circles for α and triangles for β), while solid and dashed lines are a smoothing of the data made to help the visualization of the trend for α and β respectively. The horizontal dotted lines indicate the 95% confidence level of the normal Z-score.

C.   Treatment plans

Here an exemplary case of prostate cancer is presented: figure 8 shows the distributions of dose-averaged LET (LETd) observed respectively for H, He, Li and C irradiations, while figure 9 points out the resulting β spatial modulations obtained by the integration of the MCt-MKM in the TPS. Figure 10 shows the percentage variation of the RBE expected for a protraction of the total delivery time of 10 minutes with respect to the acute irradiation. Note that to define the RBE one has to clearly identify the low LET reference radiation. In particular, for the present study, the reference radiation has be defined taking into account explicitly the dose rate time structure. For these evaluations we choose to use as a unique
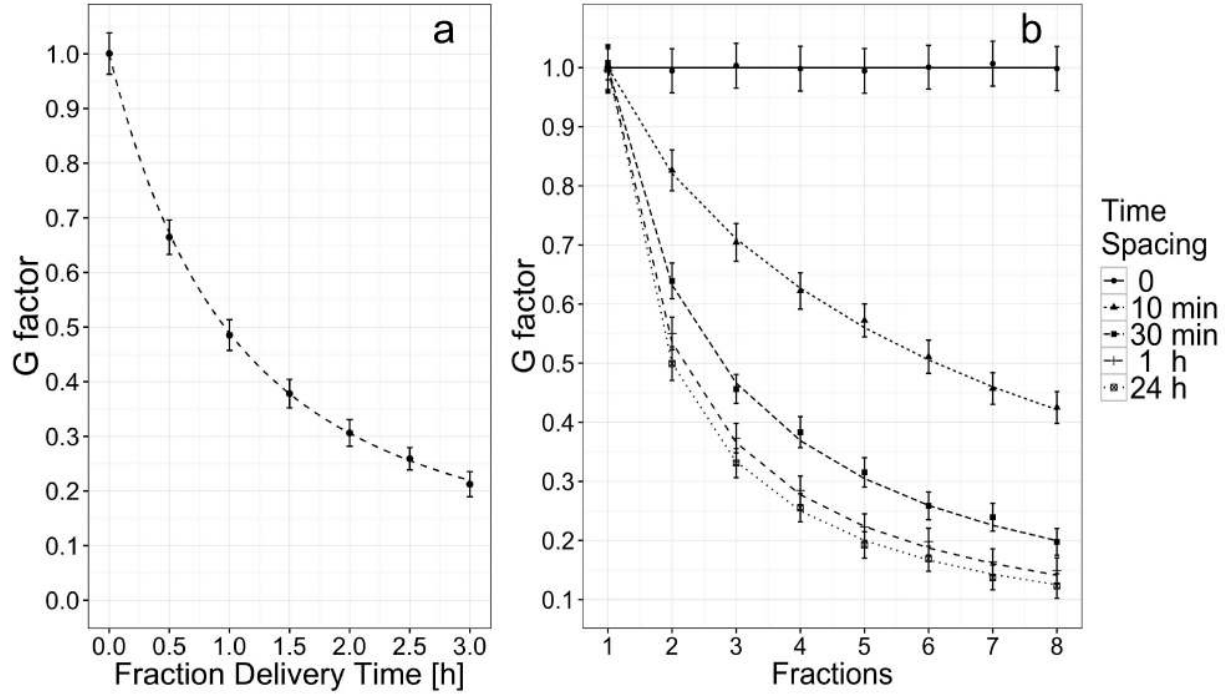
17

Figure 7. Panel a) G factor as a function of the fraction delivery time, expressed in hours. Points represent the simulated data with associated uncertainties, while the dashed line indicates the analytical calculation (equation 12). Panel b) G factor as a function of the number of fractions, with varying the time spacing between fractions. Points represent the simulated data with associated uncertainties, while lines indicate the analytical calculations (equation 13); different shapes and lines corresponds to different time spacing between fractions. The Monte Carlo data were simulated with He at 14.22 MeV/u (both panels). The legend only refers to panel b.

reference radiation an acute (instantaneously delivered) low LET irradiation, for both acute ion irradiation and protracted ion irradiation. The comparison between different primary ions indicates a higher sensitivity to the dose protraction for low-LET particles. Moreover, in the case of H and He irradiation it was observed a localization of the effect in the target volume where the dose is higher, while in the case of Li and C irradiation the higher β modulations lead to a reduced sensitivity to time protraction in the target and then a greater effect in the entrance region.
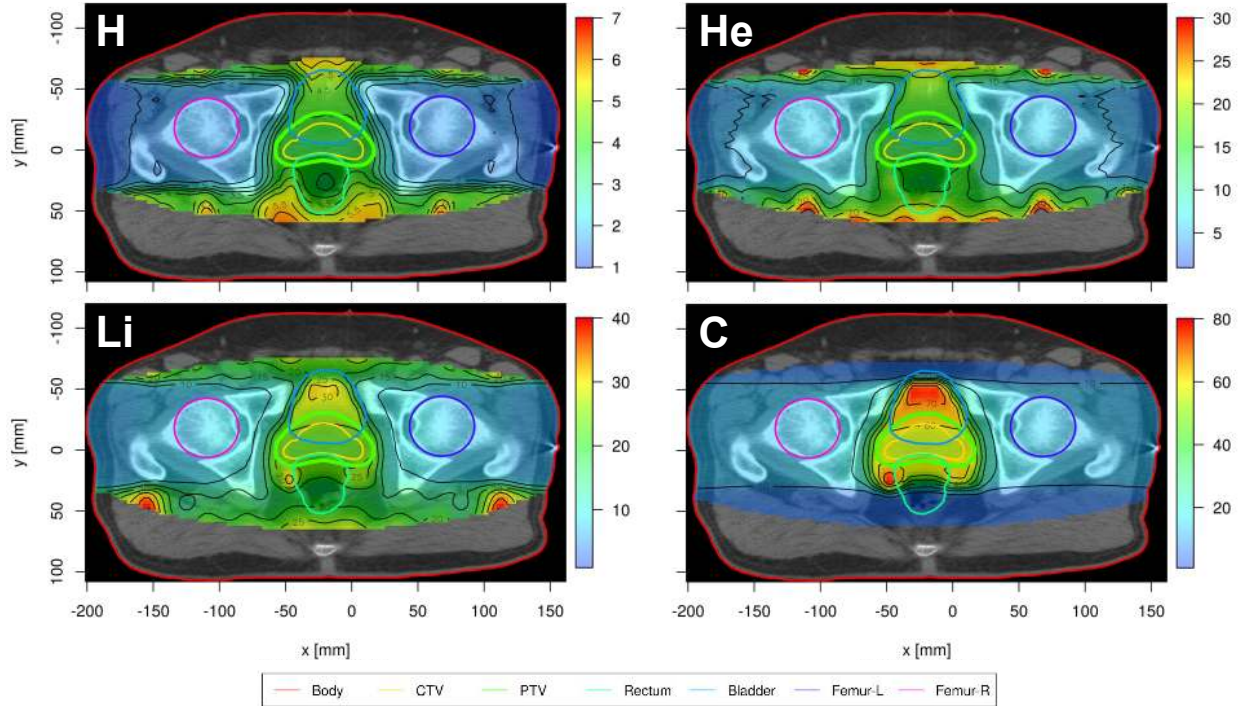
Figure 8. Prostate cancer clinical case. Dose averaged LET distributions obtained for H, He, Li and C beams irradiation, expressed in keV/μm.

IV. DISCUSSION

A. Radiobiological modeling

The results reported in section III A and a χ^2-based analysis of different models, including the LEM and the original formulation of the MKM, shows a better capability of the MCt-MKM to reproduce the experimental behaviour of both the radiobiological LQ parameters α and β. A resuming table of the χ^2 values obtained for the different models and different cell lines is also included in the supplementary material (table S I). An interesting aspect of the MCt-MKM model is that the Monte Carlo approach maintains the capability to reproduce the behaviour of different ions simultaneously, and to discriminate between them thanks to the adoption of the ion-dependent Kiefer-Chatterjee amorphous track model following the approach of Kase *et al.* [23]. The main difference with respect to the original MKM is that the MCt-MKM predicts a non constant and vanishing β with high LET values (figures 2, 3 and 4). A saturation effect is observed for both α and β parameters. Besides our MC approach, this saturation effect has been introduced in 2003 in the MKM model with
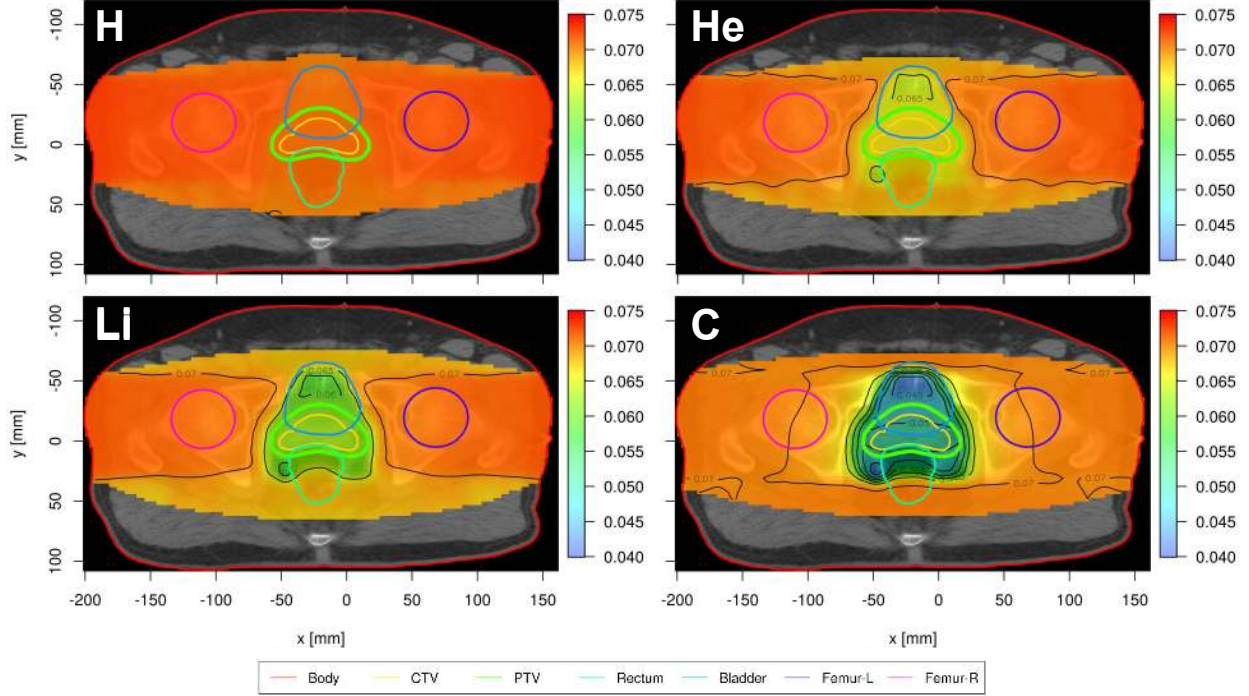
19

Figure 9.   Prostate cancer clinical case. β distributions obtained for H, He, Li and C beams irradiation, expressed in Gy^{-2}.

the non-Poissonian correction factor [22, 23]. An equivalent alternative correction method is given in [29] where a saturation-corrected specific energy factor is introduced instead. However, these LET dependent correction factors have been only evaluated explicitly for the α parameter, while a LET independence has been assumed for the β parameter.

The presented results shows that this non-Poissonian behaviour is automatically accounted for in our MC approach without the need of auxiliary correction factors. In particular, when the LET increases, less particles are needed to deliver the same macroscopic dose so that the radiation is densely ionizing and the damages will be highly localized. This sparseness causes some cell not to be affected by the radiation. Moreover only few particles are needed to kill a cell, and if some additional particle crosses the same cell they will not be effective with the exception of the first ones. This non-Poissonian behaviour is also responsible for the decreasing β. Such a decrease is caught by the Monte Carlo approach which accounts for the stochastic spatial correlations between different tracks while it is neglected in the original analytical version where a constant β is assumed. Although, as previously noted, there are still contradictory experimental results for β vs. LET behaviour [8, 12], a
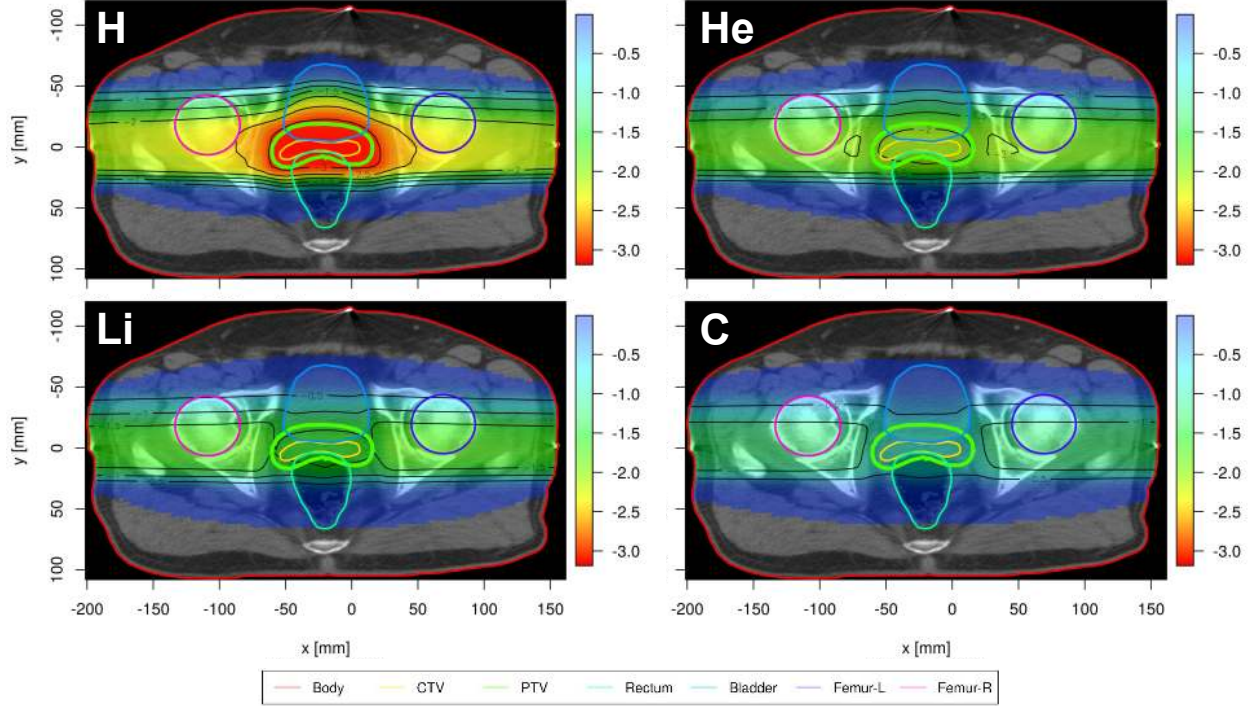
20

Figure 10. Prostate cancer clinical case. Relative percentage variation of the RBE expected for a protraction of the total delivery time of 10 minutes with respect to the acute irradiation. Values obtained for H, He, Li and C beams irradiation.

low or negligible β parameter is to be expected for high LET particle irradiation, when a single particle track has a high cell inactivation efficiency. This decreasing β behaviour can be also explained in the framework of the local effect interpretation of the MKM, in which it is the high spatially localized dose (i.e. higher specific energy deposited in few domain) of high LET particles that causes complex non repairable damages, thus reducing the efficacy of the repair mechanisms, that are usually associated to the parameter of the LQ formulation. Indeed the β evaluated with LEM shows a decreasing behaviour similar the one obtained with our MC-based MKM approach. This also highlights the analogy with the LEM [13–18].

The similarities between MKM and LEM have been already demonstrated in [23] where it has been shown that the solution of the asymptotic MKM equations is compatible with a local effect interpretation of the MKM, when an explicit track model is included in the model. The MCt-MKM approach proposed in the present work further extends the similarities between MKM and LEM, bringing a MC statistical evaluation approach to the MKM

21

evaluations similar to the one used in the original LEM formulation. In particular the MC approach is able to reproduce correctly the non-Poissonian regime also for the β parameter, that is neglected in the original MKM formulation, while it is accounted for in the LEM. Interestingly, the decrease of β predicted by the MCt-MKM seems to happen at higher LETs than the one predicted by the LEM (figures 2, 4 and 3). Nonetheless, the result is in contrast with the prediction of other models such as the repair-misrepair fixation (RMF) model [24, 42] as pointed out by Carabe-Fernandez *et al.* [33] and, although the χ^2 analysis shows a better agreement of the MCt-MKM with the experimental data, the experimental uncertainty related to the published data does not allow to exclude different scenarios.

As stated in section II, a further peculiarity of the MCt-MKM is that it provides the possibility of evaluating the temporal effect of the irradiation, intended as the variability of the cell survival and consequently of the LQ parameters deriving from the specific dose rate time structure considered (e.g. fractionation or protraction). Such a feature is validated through the comparison with the experimental data, as shown in figure 5, and provides an additional tool to compare the effect of different primary ions. This is made possible by the introduction of the analytic solution of the kinetic equations 3 formulated by Hawkins, describing the temporal evolution of the DNA damages inside the cell nucleus. It was shown (figure 6) that only the β parameter is affected by the temporal modulation and that it can be factorized as the product of a macroscopic Lea-Catcheside G factor times the β parameter identified in acute conditions. This is compatible with the local effect interpretation of the MKM introduced by Kase *et al.* [23]. Within this local effect interpretation, not only the acute effect at the micrometric level of the domains is related to the macroscopic LQ parameters of the reference low-LET radiation, but also the local repair kinetics can be inferred from the observed macroscopic low-LET behaviour. As a consequence, the resulting macroscopic G factor (equation 11) could be associated with the original definition in the case of X-ray radiation. We remark that this local effect interpretation introduces the possibility of evaluating the temporal effect of the irradiation also in the case of the LEM, despite of the lack of underlying kinetic equations in this model. Furthermore, in the case of MKM, the concept of domain can be associated with the mean autocorrelation length of the DNA damages (equation 8). This length can be experimentally measured by means of immunofluorescence techniques using DNA damage markers (e.g. γ-H2AX) [43]. Note that the obtained Lea-Catcheside factor is characterized by a first order exponential repair

kinetics as direct consequence of the formulation chosen for the kinetic equations 3.

Actually, the scientific community is divided about this subject and several authors suggest the possibility of considering different repair pathways leading to multi-exponential repair law [44], or terms at the second order resulting in non-exponential laws such as the hyperbolic solution introduced by Carabe-Fernandez *et al.* [45]. This leaves room for future developments by introducing in the proposed model different repair kinetics formulations in the framework of the local effect assumptions.

B. Clinical case

As pointed out in figures 8, 9 and 10 a strong correlation occurs between the distribution of the physical quantities (such as the dose or the LETd), the LQ radiobiological parameters and the dose rate time structure, also depending on the chosen ion, so that the biological effectiveness of the treatment cannot be easily predicted. By means of the MCt-MKM it was shown that the temporal effect is mediated exclusively by the quadratic terms of the LQ relation (figure 6) and figures 8, 9 and 10 highlight a complex interplay between the physical dose, the LET of the irradiation, the β parameter and the RBE. In particular, the expected decrease of effectiveness for time protraction is stronger in the target where the dose is higher, but it is slighter with increasing the charge of the particle used due to the lower β resulting from the increased LET (figure 8), in agreement with the MCt-MKM predictions. This seems to suggest that the protons represent the best choice for a hypofractionated treatment because of the flatten β distribution. Such an effect is minimized in the case of carbon ions whose sensitivity to the dose rate time structure is inhibited in the high LET region. Note that, as suggested by equations 12 and 13, the temporal effect of the irradiation depends on the value of the repair constant τ, which has been experimentally extrapolated by the split-dose data (section II). These issues become relevant when thinking about a clinical application of the model. For this purpose a sensitivity analysis of the cell survival to this parameter has been carried out and reported in figure 5. An analysis of the impact of τ variations to the average RBE for different protraction scenarios (from 0 to 1 hour) has also been carried out and reported in the supplementary material (figure S5). These preliminary analyses show a good robustness of the model to the specific choice of the τ parameter. It is also mandatory to emphasize that these results are intrinsically influenced by the model

23

used and, even though it is compatible with the published experimental data, it is impossible to exclude different scenarios arising from the application of other models. We remark that the main purpose of this study was to investigate the effects of dose-delivery time structure on biological effectiveness in ion beam therapy. In particular, we focused on the modelling of the repair kinetics mechanism of the cell, neglecting other time related radiobiological mechanisms that are clinically relevant, such as the tumor repopulation dynamics. A further limit of the modelization is that it considers cell survival as the only biological endpoint.

V. CONCLUSIONS

A new model was presented to better reproduce the variability of the LQ parameters as a function of the particle LET. The Monte Carlo approach to the MKM allows to account for the stochastic nature of the irradiation process, leading to a higher precision in the estimation of the quadratic β parameter which modulates the temporal effect of the irradiation. In the case of acute irradiation, the model was validated through the comparison with the experimental data collected in the PIDE, while the data of a split-dose experiment were used to experimentally define the value of the time constant characteristic of the repair kinetics. The model has been included in the TPS and used to analyse a case of prostate cancer irradiated with different primary ions with a protracted dose delivery. A complex interconnection was found between the physical and radiobiological quantities, which certainly needs further and more detailed studies. In this context, the MCt-MKM provides a new tool to optimize treatment plans with a better control of the radiobiological quantities and to evaluate the effect of using different sources and advanced delivery techniques with complex dose rate time structures, such as repainting or respiratory gating.

Appendix A: Solution of the kinetic equations

The solution of the kinetic equations (3) represents one of the key points of the MCt-MKM. This appendix is intended to drive the reader in the solution of these equations, clarifying the passages that leads from equation 3 to equation 6.

Consider a cell from a population exposed to irradiation at the time $t = 0$ and a domain absorbing z in the interaction with an ion. Then, according to equation 3, it is possible to

24

define the boundary conditions:

$$\begin{cases} x_I^{(cd)}(t=0) = \lambda\, z^{(cd)} \\ x_{II}^{(cd)}(t=0) = k\, z^{(cd)} \end{cases} \tag{A1}$$

The indexes c and d refers to the cell and the domain: from now they will be omitted to make the equation more readable. In this case the solution of the kinetic equation for x_{II} is a simple exponential, which imply:

$$\begin{cases} x_I(t) = \lambda z + \int_0^t \left[a\, kz\, e^{-(a+r)t'} + b\, k^2 z^2\, e^{-2(a+r)t'} \right] dt' \\ x_{II}(t) = kz\, e^{-(a+r)t} \end{cases} \tag{A2}$$

where the integral defining x_I can be easily solved, resulting (in the limit of $t \to \infty$) in:

$$x_I = \left(\lambda + \frac{ak}{a+r} \right) z + \left(\frac{bk^2}{2(a+r)} \right) z^2 \tag{A3}$$

which highlights the linear and quadratic components of the lethal damages. This process needs to be generalized to consider a sequence of n consecutive interactions occurring at the times $\{t_0, t_1, \dots, t_{n-1}\}$, in which the domain absorbs $\{z_0, z_1, \dots, z_{n-1}\}$. The solution of equation 3 for x_{II}, in this case, has to be split in n time intervals:

$$x_{II}(t) = \begin{cases} kz_0 \exp\left[-(a+r)(t-t_0)\right] \equiv x_{II}^{(0)} & t_0 < t < t_1 \\ kz_0 \exp\left[-(a+r)(t-t_0)\right) + kz_1 \exp\left(-(a+r)(t-t_1)\right] \equiv x_{II}^{(1)} & t_1 < t < t_2 \\ \quad\vdots & \vdots \\ \displaystyle\sum_{i=0}^{n-2} kz_i \exp\left[-(a+r)(t-t_i)\right] \equiv x_{II}^{(n-2)} & t_{n-2} < t < t_{n-1} \\ \displaystyle\sum_{i=0}^{n-1} kz_i \exp\left[-(a+r)(t-t_i)\right] \equiv x_{II}^{(n-1)} & t > t_{n-1} \end{cases} \tag{A4}$$

The integral defining x_I (equation A2) has to be split as well in n integrals:

$$x_I(t) = \sum_{i=0}^{n-2} \left[\lambda z_i + \int_{t_i}^{t_{i+1}} \left(ax_{II}^{(i)} + bx_{II}^{(i)^2} \right) dt \right] + \lambda z_{n-1} + \int_{t_{n-1}}^{t} \left(ax_{II}^{(n-1)} + bx_{II}^{(n-1)^2} \right) dt' \tag{A5}$$

which can be solved in the same way of A2, in the limit of $t \to \infty$, leading to:

$$x_I = \frac{\alpha_0}{N_D} \sum_{i=0}^{n-1} z_i + \frac{\beta_0}{N_D} \sum_{i=0}^{n-1} z_i^2 + \frac{\beta_0}{N_D} \sum_{i=0}^{n-2} \sum_{j=i+1}^{n-1} e^{-(a+r)(t_j-t_i)} 2z_i z_j \tag{A6}$$

25

being:

$$\begin{cases} \dfrac{\alpha_0}{N_D} = \lambda + \dfrac{ak}{a+r} \\ \dfrac{\beta_0}{N_D} = \dfrac{bk^2}{2(a+r)} \end{cases} \quad . \tag{A7}$$

Equation 6 can be obtained by subtracting and adding to equation A6 the quantity:

$$\frac{\beta_0}{N_D} \sum_{i=0}^{n-2} \sum_{j=i+1}^{n-1} 2z_i z_j \quad . \tag{A8}$$

Disclosure of conflict of interest

The authors declare that they do not have any conflict of interest.

---

[1] B. Jones, "The case for particle therapy," The British Journal of Radiology **79**, 24–31 (2006).

[2] T. Lomax and C.-M. Charlie Ma, *Proton and carbon ion therapy*, Imaging in medical diagnosis and therapy (Taylor & Francis, 2013).

[3] B. Jones, T.S.A. Underwood, and R.G. Dale, "The potential impact of relative biological effectiveness uncertainty on charged particle treatment prescriptions," The British Journal of Radiology **84**, S061–S069 (2011).

[4] R.G. Dale, B. Jones, and A. Carabe-Fernandez, "Why more needs to be known about the RBE effects in modern radiotherapy," Applied Radiation and Isotopes **67**, 387–392 (2009).

[5] D. E. Lea and D. G. Catcheside, "The mechanism of the induction by radiation of chromosome aberrations in Tradescantia," Journal of Genetics **44**, 216–245 (1942).

[6] D. E. Lea, *Actions of Radiation on Living Cells* (Cambridge University Press, London, 1946).

[7] D. J. Brenner, L. R. Hlatky, P. J. Hahnfeldt, Y. Huang, and R. K. Sachs, "The linear-quadratic model and most other common radiobiological models result in similar predictions of time-dose relationships," Radiation Research **150**, 83–91 (1998).

[8] T. Friedrich, U. Scholz, T. Elsasser, M. Durante, and M. Scholz, "Systematic analysis of RBE and related quantities using a database of cell survival experiments with ion beam irradiation," Journal of Radiation Research **54**, 494–514 (2012).

[9] K. Ando, S. Koike, K. Nojima, Y.J. Chen, C. Ohira, N. Ando, T. Kobayashi, W. Ohbuchi, T. Shimizu, and K. Kanai, "Mouse skin reactions following fractionated irradiation with carbon ions," International Journal of Radiation Biology **74**, 129–138 (1998).

[10] K. Ando, S. Koike, A. Uzawa, N. Takai, T. Fukawa, Y. Furusawa, M. Aoki, and Y. Miyato, "Biological gain of carbon-ion radiotherapy for the early response of tumor growth delay and against early response of skin reaction in mice," Journal of Radiation Research **46**, 51–57 (2005).

[11] M. Zaider, "The variation of β with radiation quality in the α/β model," Radiation Research **141**, 228–230 (1995).

[12] F. Guan, L. Bronk, U. Titt, S.H. Lin, D. Mirkovic, M.D. Kerr, X.R. Zhu, J. Dinh, M. Sobieski, C. Stephan, C.R. Peeler, R. Taleei, R. Mohan, and D.R. Grosshans, "Spatial mapping of the biologic effectiveness of scanned particle beams: towards biologically optimized particle therapy," Scientific reports **5** (2015), 10.1038/srep09850.

[13] M. Scholz and G. Kraft, "Track structure and the calculation of biological effects of heavy charged particles," Advances in Space Research **18**, 5–14 (1996).

[14] M. Scholz, A.M. Kellerer, W. Kraft-Weyrather, and G. Kraft, "Computation of cell survival in heavy ion beams for therapy," Radiation and Environmental Biophysics **36**, 59–66 (1997).

[15] T. Elsässer and M. Scholz, "Improvement of the local effect model (LEM) implications of clustered DNA damage," Radiation Protection Dosimetry **122**, 475–477 (2006).

[16] T. Elsässer and M. Scholz, "Cluster effects within the local effect model," Radiation Research **167**, 319–329 (2007).

[17] T. Elsässer, M. Krämer, and M. Scholz, "Accuracy of the local effect model for the prediction of biologic effects of carbon ion beams in vitro and in vivo," International Journal of Radiation Oncology*Biology*Physics **71**, 866–872 (2008).

27

[18] T. Elsässer, W.K. Weyrather, T. Friedrich, M. Durante, G. Iancu, M. Krämer, G. Kragl, S. Brons, M. Winter, K.J. Weber, and M. Scholz, "Quantification of the relative biological effectiveness for ion beam radiotherapy: direct experimental comparison of proton and carbon ion beams and a novel approach for treatment planning," International Journal of Radiation Oncology*Biology*Physics **78**, 1177–1183 (2010).

[19] R.B. Hawkins, "A statistical theory of cell killing by radiation of varying Linear Energy Transfer," Radiation Research **140**, 366–374 (1994).

[20] R.B. Hawkins, "A Microdosimetric-Kinetic Model of cell death from exposure to ionizing radiation of any LET, with experimental and clinical applications," International Journal of Radiation Biology **69**, 739–755 (1996).

[21] R.B. Hawkins, "A microdosimetric-kinetic theory of the dependence of the RBE for cell death on LET," Medical Physics **25**, 1157–1170 (1998).

[22] R.B. Hawkins, "A Microdosimetric-Kinetic Model for the effect of non-Poisson distribution of lethal lesions on the variation of RBE with LET," Radiation Research **160**, 61–69 (2003).

[23] Y. Kase, T. Kanai, N. Matsufuji, Y. Furusawa, T. Elsässer, and M. Scholz, "Biophysical calculation of cell survival probabilities using amorphous track structure models for heavy-ion irradiation," Physics in Medicine and Biology **53**, 37–59 (2008).

[24] D.J. Carlson, R.D. Stewart, V.A. Semenenko, and G.A. Sandison, "Combined use of Monte Carlo DNA damage simulations and deterministic repair models to examine putative mechanisms of cell killing," Radiation Research **169**, 447–459 (2008).

[25] M. Krämer and M. Scholz, "Treatment planning for heavy-ion radiotherapy: calculation and optimization of biologically effective dose," Physics in Medicine and Biology **45**, 3319–3330 (2000).

[26] I. Schlampp, C.P. Karger, O. Jäkel, M. Scholz, B. Didinger, A. Nikoghosyan, A. Hoess, M. Krämer, L. Edler, J. Debus, and D. Schulz-Ertner, "Temporal lobe reactions after radiotherapy with carbon ions: incidence and estimation of the relative biological effectiveness by the local effect model," International Journal of Radiation Oncology*Biology*Physics **80**, 815–823 (2011).

[27] P. Fossati, S. Molinelli, N. Matsufuji, M. Ciocca, A. Mirandola, A. Mairani, J. Mizoe, A. Hasegawa, R. Imai, T. Kamada, R. Orecchia, and H. Tsujii, "Dose prescription in carbon ion radiotherapy: a planning study to compare nirs and lem approaches with a clinically-

560 oriented strategy," Physics in medicine and biology **57**, 7543–7554 (2012).

[28] S.E. Combs, K.A. Kessel, K. Herfarth, A. Jensen, S. Oertel, C. Blattmann, S. Ecker, A. Hoess, E. Martin, O. Witt, O. Jäkel, A.E. Kulozik, and J. Debus, "Treatment of pediatric patients and young adults with particle therapy at the Heidelberg Ion Therapy center (HIT): establishment of workflow and initial clinical data," Radiation Oncology **7**, 1 (2012).

565 [29] T. Inaniwa, T. Furukawa, Y. Kase, N. Matsufuji, T. Toshito, Y. Matsumoto, Y. Furusawa, and K. Noda, "Treatment planning for a scanned carbon beam with a modified microdosimetric kinetic model," Physics in Medicine and Biology **55**, 6721–6737 (2010).

[30] F. Kamp, G. Cabal, A. Mairani, K. Parodi, J.J. Wilkens, and D.J. Carlson, "Fast biological modeling for voxel-based heavy ion treatment planning using the mechanistic repair-

570 misrepair-fixation model and nuclear fragment spectra," International Journal of Radiation Oncology*Biology*Physics **93**, 557–568 (2015).

[31] T. Inaniwa, M. Suzuki, T. Furukawa, Y. Kase, N. Kanematsu, T. Shirai, and R.B. Hawkins, "Effects of dose-delivery time structure on biological effectiveness for therapeutic carbon-ion beams evaluated with microdosimetric kinetic model," Radiation Research **180**, 44–59 (2013).

575 [32] T. Inaniwa, N. Kanematsu, M. Suzuki, and R.B. Hawkins, "Effects of beam interruption time on tumor control probability in single-fractionated carbon-ion radiotherapy for non-small cell lung cancer," Physics in Medicine and Biology **60**, 105–121 (2015).

[33] A. Carabe-Fernandez, R.G. Dale, J.W. Hopewell, B. Jones, and H. Paganetti, "Fractionation effects in particle radiotherapy: implications for hypo-fractionation regimes," Physics in

580 Medicine and Biology **55**, 5685–5700 (2010).

[34] A.M. Kellerer and H.H. Rossi, "A generalized formulation of dual radiation action," Radiation Research **75**, 471–488 (1978).

[35] M. Zaider and H.H. Rossi, "The synergistic effects of different radiations," Radiation Research **83**, 732–739 (1980).

585 [36] C.A. Tobias, "The repair-misrepair model in radiobiology: Comparison to other models," Radiation Research **104**, S77–S95 (1985).

[37] S.B. Curtis, "Lethal and potentially lethal lesions induced by radiation—a unified repair model," Radiation Research **106**, 252–270 (1986).

[38] J. Kiefer and H. Straaten, "A model of ion track structure based on classical collision dynamics

590 (radiobiology application)," Physics in Medicine and Biology **31**, 1201–1209 (1986).

29

[39] A. Chatterjee and H. J. Schaefer, "Microdosimetric structure of heavy ion tracks in tissue," Radiation and Environmental Biophysics **13**, 215–227 (1976).

[40] G. Russo, A. Attili, G. Battistoni, D. Bertrand, F. Bourhaleb, F. Cappucci, M. Ciocca, A. Mairani, F.M. Milian, S. Molinelli, M.C. Morone, S. Muraro, T. Orts, V. Patera, P. Sala, E. Schmitt, G. Vivaldo, and F. Marchetto, "A novel algorithm for the calculation of physical and biological irradiation quantities in scanned ion beam therapy: the beamlet superposition approach," Physics in Medicine and Biology **61**, 183–214 (2016).

[41] A. Ferrari, P.R. Sala, A. Fasso, and J. Ranft, *FLUKA: A multi-particle transport code (Program version 2005)*, Tech. Rep. (2005).

[42] M.C. Frese, V.K. Yu, R.D. Stewart, and D.J. Carlson, "A mechanism-based approach to predict the relative biological effectiveness of protons and carbon ions in radiation therapy," International Journal of Radiation Oncology*Biology*Physics **83**, 442–450 (2012).

[43] G. Schettino, M. Ghita, D.J. Richard, and K.M. Prise, "Spatio temporal investigations of DNA damage repair using microbeams," Radiation protection dosimetry **143**, 340–343 (2011).

[44] E. Dikomey and J. Franzke, "DNA repair kinetics after exposure to X-irradiation and to internal β-rays in CHO cells," Radiation and Environmental Biophysics **25**, 189–194 (1986).

[45] A. Carabe-Fernandez, R.G. Dale, and H. Paganetti, "Repair kinetic considerations in particle beam radiotherapy," British Journal of Radiology **84**, 546–555 (2011).